Drosophila Nuclear Receptor E75 Is a Thiolate Hemoprotein†

Eve de Rosny,*,‡ Arjan de Groot,§ Celine Jullian-Binard,‡ Jacques Gaillard,|| Franck Borel,‡ Eva Pebay-Peyroula,‡ Juan Carlos Fontecilla-Camps,‡ and Hélène M. Jouve‡

CEA, CNRS, UJF, UMR 5075, Institut de Biologie Structurale Jean-Pierre Ebel, 41 rue Jules Horowitz, 38027 Grenoble Cedex 1, France, CEA, DSV, DEVM, LEMIRE, UMR 6191 CNRS/CEA/Aix Marseille Univ, F-13108 Saint Paul Lez Durance, France, and SCIB, UMR E3-CEA/UJF, Département de Recherche Fondamentale sur la Matière Condensée, CEA-Grenoble, 17 rue des Martyrs, F-38054 Grenoble Cedex 9, France

Received March 17, 2006; Revised Manuscript Received June 19, 2006

ABSTRACT: *Drosophila* E75 is a member of the nuclear receptor superfamily. These eukaryotic transcription factors are involved in almost all physiological processes. They regulate transcription in response to binding of rigid hydrophobic hormone ligands. As it is the case for many nuclear receptors, the E75 hormone ligand was originally unknown. Recently, however, it was shown that the ligand binding domain (LBD) of E75 contains a tightly bound heme prosthetic group and is gas responsive. Here we have used site-directed mutagenesis along with UV−visible and electron paramagnetic resonance (EPR) spectroscopies to characterize and assign the heme iron axial ligands in E75. The F370Y mutation and addition of hemin to the growth medium during expression of the protein in *Escherichia coli* were necessary to produce good yields of heme-enriched E75 LBD. EPR studies revealed the presence of several species containing a strongly iron bound thiolate. The involvement of cysteines 396 and 468 in heme binding was subsequently shown by single and double mutations. Using a similar approach, we have also established that the sixth iron ligand of a well-defined coordination conformation, which accounts for approximately half of the total species, is histidine 574. The other iron coordination pairs are discussed. We conclude that E75 is a new example of a thiolate hemoprotein and that it may be involved in hormone synthesis regulation.

Nuclear receptors, the largest superfamily of eukaryotic transcription factors, are involved in almost all physiological processes. They regulate transcription in response to binding of lipophilic hormone ligands such as steroids, thyroid hormones, retinoic acid in mammalian cells, and ecdysone in insect cells. They contain three main functional domains: (i) N-terminal domain A/B, which is highly variable in length and sequence and which has a constitutively active transactivation function, (ii) the DNA binding domain (DBD)[1] specific to DNA nucleotide motifs, and (iii) the ligand binding domain (LBD), which is involved not only in binding of the hormone ligand but also in dimerization and binding to coregulator proteins (corepressors and coactivators). It has been proposed that binding of the hormone ligand to the LBD induces conformational changes mainly affecting the orientations of three helices (H3, H11, and H12) of the LBD. These conformational changes trigger the displacement of a corepressor protein and the recruitment of a coactivator protein, resulting in transcription activation (*1*). However, other mechanisms are probably involved because many hormone ligands function as agonists in certain tissues and antagonists in others. Moreover, it has been shown that transcription can be regulated by heterodimerization. For example, the *Drosophila* E75B isoform, which does not contain a DBD, can heterodimerize with DHR3 and thereby block the ability of DHR3 to induce the expression of nuclear receptor βFTZ-F1 (*2*). The crystal structures of approximately 15 different LBDs have been determined, most of them in complex with either natural or synthetic hormone ligands. Only three of these are from *Drosophila* or other insect nuclear receptors. The LBD structure is highly conserved with a fold containing 11−12 helices and one β-hairpin (*1*) and contains a topologically conserved ligand binding pocket (LBP). Indeed, residues found in the LBP occupy conserved positions in the homology sequence alignments and, by extension, in the three-dimensional structures. It is the nature of these residues that determines both LBP size and hormone ligand specificity (*1*).

All known nuclear receptor hormone ligands are small, fairly rigid, and very hydrophobic (*3*) and display high affinities for their cognate nuclear receptor with K_d values usually in the nanomolar range (*3*−*5*). However, the majority

† This work was supported by Genopole Rhone-Alpes.

* To whom correspondence should be addressed: LCCP, Institut de Biologie Structurale (UMR 9015), 41 rue Jules Horowitz, 38027 Grenoble Cedex 1, France. Telephone: 33 (4) 38 78 59 24. Fax: 33 (4) 38 78 54 94. E-mail: eve.derosny@ibs.fr.

‡ CEA, CNRS, UJF, UMR 5075.

§ CEA, DSV, DEVM, LEMIRE, UMR 6191 CNRS/CEA/Aix Marseille Univ.

|| CEA-Grenoble.

[1] Abbreviations: DBD, DNA binding domain; LBD, ligand binding domain; DHR3, *Drosophila* hormone receptor 3; LBP, ligand binding pocket; PAS, acronym of period protein (PER), aryl hydrocarbon receptor nuclear translocator protein (ARNT), and single-minded protein (SIM); HRI, heme-regulated eIF2α kinase; CooA, CO oxidation activator protein from *Rhodospirillum rubrum*; HRM, heme responsive motif; UV, ultraviolet; EPR, electron paramagnetic resonance; CBS, cystathionine β-synthase; SoxAX, multiheme enzyme encoded by the *SoxA* gene; Trx, thioredoxin; MBP, maltose binding protein; GST, glutathione *S*-transferase; REV, hRev-erbAα; sE75, soluble E75 ligand binding domain; Rz, Reinheitszahl index; CPO, chloroperoxidase; P450, cytochrome P450; eNOS, endothelial nitric oxide synthase; preALAS-E, precursor of the erythroid δ-aminolevulinic synthase.

10.1021/bi060537a CCC: $33.50
Published on Web 07/25/2006

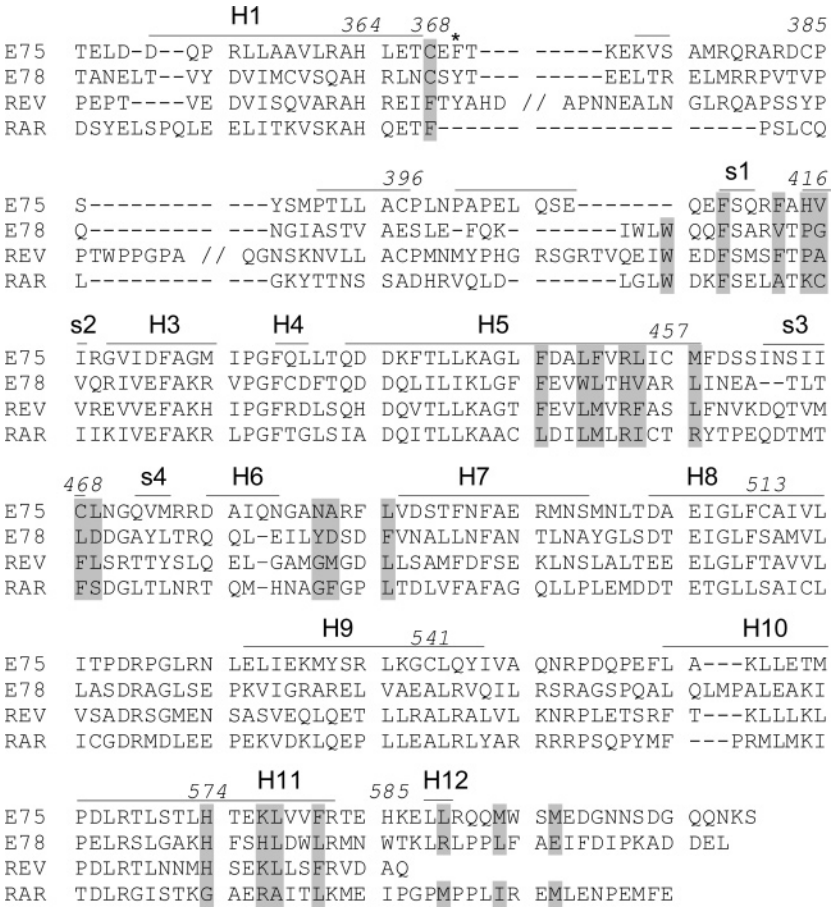

FIGURE 1: Sequence alignment of E75, E78, hRev-erbAα (REV), and hRARγ (RAR) ligand binding domains. The REV and RAR alignment is from ref *32*. E75 and E78 alignments with REV were created using the MultAlign sequence alignment server. Numbers in italics above E75 cysteines and histidines are based on the *Drosophila* E75A sequence. The ligand binding pocket (LBP) residues of the crystallized RAR (PDB entry 2LBD) and their putative counterparts in E75, E78, and REV are shaded. Double slashes represent sequence interruptions in long REV unconserved domains. Thin lines represent E75 secondary structures found by the structure homology server Swiss-model; helix (H) numbering is based on the RAR structure. s*x* labels indicate β-strands. Asterisks denote the position of the F370 mutated to a tyrosine in sE75.

of nuclear receptors are orphan, meaning that their natural hormone ligand, if it exists, has not been identified. The identification of new ligands has major implications in our understanding of biological mechanisms such as development, reproduction, and cell functions. It can also lead to the discovery of both new drugs for the treatment of human diseases and novel specific and environment-friendly insecticides.

E75 was thought originally to be an orphan nuclear receptor. Very recently, however, Reinking and collaborators (*6*) showed that E75 contains a heme prosthetic group that binds NO and CO. On the basis of this result, they proposed that E75 may be a gas sensor. E75 is the first nuclear receptor found to belong to the hemoprotein class. Hemoproteins are involved in numerous fundamental biological processes such as the transport and storage of oxygen, redox reactions, electron transfer, and nitric oxide transport. More recently, it has been shown that heme can also act as a biosensor for gaseous ligands such as NO, CO, and O_2, in enzymes, and in transcription factors containing PAS domains (*7*). These members of the PAS family share a predictable α/β three-dimensional fold of ~130 residues (*8*) not found in nuclear receptor structures. In most of the gas sensor hemoproteins, the proximal axial amino acid residue is a histidine but two non-PAS thiolate hemoproteins, HRI (Cys/His coordination) (*9*) and CooA (Cys/Pro coordination) (*10*), have also recently been found. The few other known heme−thiolate proteins are enzymes such as P450, chloroperoxidase, cystathionine-β-synthase (CBS), and nitric oxide synthase (eNOS) that catalyze various reactions, including oxygenations, oxidations, reductions, isomerizations, and dehydrations (*11*). In addition to its role as a prosthetic group, heme can be itself a signaling molecule. Notably, it regulates the activity of yeast transcription factor HAP (*12*) and mammalian transcription factor Bach1 (*13*). These proteins, which are directly regulated via heme binding, contain several conserved heme responsive motifs (HRMs). HRMs consist of two or more invariable Cys-Pro sequences surrounded by four or five fewer conserved residues (*12*, *14*, *15*). They bind heme reversibly with affinities in the micromolar range. Interestingly, E75 contains two Cys-Pro motifs (Figure 1), suggesting that heme may be a signaling molecule like all other described nuclear receptor hormone ligands. To date, the heme iron coordination of E75 has not been clearly elucidated. Reinking and collaborators (*6*) proposed that either H364 or H574 is an axial ligand to iron, but no substantial evidence was provided because they did not succeed in expressing the corresponding mutated proteins. Determination of which E75 residues are involved in iron binding is still needed, as it will help in our understanding of the

function of the heme, whether heme itself or a gas ligand to heme triggers the regulation of transcription by this nuclear receptor.

In this work, we report UV−visible and EPR spectroscopic and site-directed mutagenesis studies aimed at determining which LBD residues are involved in heme iron coordination. Our data show that the heme is of the *b* type with a low-spin hexacoordinated ferric iron. In addition, several iron trans coordination pairs, all containing a strongly bound cysteine, were identified. Cysteines 396 and 468 and histidine 574 were shown to be involved in these iron coordinations. We conclude that E75, along with CBS (*16*), SoxAX (*17*), and HRI (*9*), is a new addition to the few examples of Cys/His hemoproteins.

MATERIALS AND METHODS

Cloning and Site-Directed Mutagenesis. The DNA encoding the E75 LBD was amplified using poly(A+) RNA extracted from *Drosophila* embryos (12−16 h) as a template. An oligonucleotide (5′-CGGGATCCTTACGACTTGTTCTGCTGGC, BamHI site underlined) representing the QQNKS sequence (amino acids 605−609) was used for RT-PCR according to the Superscript II (Life technologies) protocol. The reverse transcriptase was inactivated by heating at 70 °C for 15 min, prior to addition of the oligonucleotide (5′-GGAATTCCATATGACCGAGCTGGATGACCA, NdeI site underlined) representing the TELDD sequence (amino acids 348−352). PCR was performed using *Pfu* polymerase. The purified PCR product was first cloned in a TOPO TA cloning vector (Invitrogen) and then in pSKB3 (gift from J. P. Renaud, Strasbourg, France) using the NdeI and BamHI restriction sites. Plasmid pSKB3 is a pET28 derivative allowing expression of proteins with an N-terminal His tag that can be removed by TEV protease. Site-directed mutageneses were performed following the QuikChange protocol (Stratagene). The F370 codon was changed for tat (Tyr). H364, H574, H585, and C385 codons were changed for gcc (Ala). The H416 codon was changed for gca (Ala). C368, C396, and C468 codons were changed for gct (Ala). All constructs were confirmed by DNA sequencing and introduced into the *Escherichia coli* BL21(DE3) strain.

Expression and Purification. Cells were grown in LB medium, in the presence or absence of 5 μM hemin, to an absorbance (A_{600}) of 0.8−1 prior to induction for 15 h at 16 °C by the addition of 0.5 mM IPTG. After centrifugation, the cell pellet was resuspended in 50 mM Tris-HCl (pH 8), 300 mM NaCl, and 15 mM imidazole plus Complete EDTA-free antiprotease (Roche Applied Sciences) and lysed in a French press. All the E75 mutants were purified by cobalt affinity column chromatography (Clontech) using a 15 to 300 mM imidazole gradient, and the E75 proteins were eluted at 150 mM imidazole. The next step was gel filtration on a High Load 16/60 Superdex 75 prep grade column (Amersham Biosciences) equilibrated and eluted with 50 mM Tris-HCl (pH 8) and 300 mM NaCl. The apparent molecular weight of the F370Y mutant protein (hereafter called sE75) was evaluated using BSA and DNase I from bovine pancreas (Roche Applied Sciences) as standards.

Determination of Extinction Coefficients and Percentages of Heme-Bound Proteins. A heme-saturated sample of sE75 was divided into two parts. One part was used for the determination of protein concentrations by quantitative amino acid analysis and the other for the determination of heme content. Amino acid analysis was performed, in triplicate, on samples dried and hydrolyzed at 110 °C in constantly boiling HCl containing 1% (v/v) phenol, for 24 h under reduced pressure and in the absence of oxygen. Amino acids were analyzed on a model 7300 Beckman amino acid analyzer, with the standard sodium citrate eluting buffer system. Calibrations were carried out with aliquots of four standard solutions, each of which contained all the amino acids except tryptophan. Heme content was determined by the pyridine hemochromogen assay, using the difference in absorbance at 556 and 580 nm, measured on the redox difference spectrum using a $\Delta(\Delta\epsilon^{red/ox})_{556-580}$ of 29 mM^{-1} cm^{-1} (*18*). After determination of the extinction coefficient (see Results), the percentages of heme-bound (holoprotein) versus the total amount of sE75 (apoprotein + holoprotein) were calculated on the basis of the following equations:

$$C_{holo} = A_{424}/\epsilon_{holo424}$$

$$C_{apo} = [A_{280} - (\epsilon_{holo280}A_{424})/\epsilon_{holo424}]/\epsilon_{apo280}$$

The H574A mutant, in the absence of imidazole, exhibited a UV−visible spectrum different from that of sE75 but exhibited similar absorption properties upon addition of 300 mM imidazole in 50 mM Tris-HCl (pH 8), 300 mM NaCl buffer. Consequently, the concentration of the holo H574A mutant was measured in the presence of imidazole using sE75 extinction coefficients. The mean value was calculated from four different H574A purified mutant protein samples.

Optical Absorption Spectra, Mass Spectrometry, and EPR Spectra. Optical spectra were recorded at room temperature, or at a regulated temperature when mentioned, in a Beckman DU 640 UV−visible spectrophotometer equipped with a cryostat. Continuous-wave (CW) EPR spectra were recorded at a low temperature (10 K) with an X-band EMX Bruker spectrometer equipped with an Oxford Instruments ESR 900 helium flow cryostat. Before being frozen, 8% (v/v) glycerol as a cryoprotectant was added to all the samples.

RESULTS

Overexpression of a Soluble E75 LBD. The E75 LBD constructs (amino acids 348−609, Figure 1) fused with either His_6, Trx, MBP, or GST tags were initially overexpressed in *E. coli* as inclusion bodies, and therefore, a mutagenesis strategy was used to increase their solubility. F370 was mutated to a tyrosine, as found in the aligned sequences of E75 homologues hRev-erbAα (REV) and E78 (Figure 1). This hydrophobic residue was selected because it was at the surface in a three-dimensional model of the E75 LBD generated by the protein structure homology modeling server Swiss-model (*19*). The F370Y LBD mutant protein was soluble in the cell lysate and could be easily purified by two chromatography steps (IMAC and gel filtration). The gel filtration chromatogram of sE75 (for the soluble E75 LBD), overexpressed with 5 μM hemin in the LB growth medium, displayed one major peak corresponding to an apparent mass of approximately 33 000 Da that contained pure sE75 as shown by SDS−PAGE (Figure 2). These data indicate that sE75 is expressed as a monomer. The expected mass of

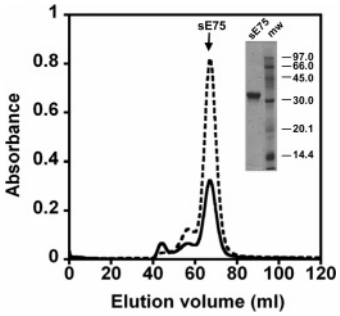

FIGURE 2: Purification of sE75. The sE75 protein was overexpressed in *E. coli* with hemin added to the LB growth medium. Gel filtration of sE75 after elution from a cobalt affinity column; a High Load 16/60 Superdex 75 prep grade column (Amersham Biosciences) equilibrated with 50 mM Tris-HCl (pH 8) and 300 mM NaCl; flow rate of 1 mL/min; $\lambda = 280$ nm (—) and $\lambda = 424$ nm (•••). The mw lane contained molecular weight markers.

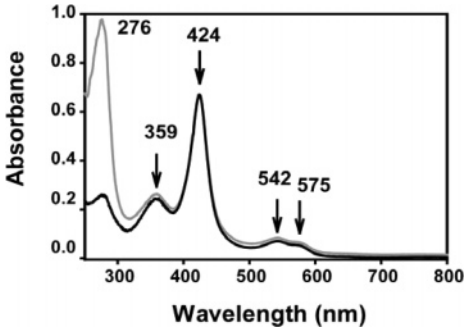

FIGURE 3: UV−visible absorption spectra of sE75. The sE75 protein was purified from *E. coli* grown in LB medium with (black line) or without (gray line) 5 μM hemin. Absorption was measured at room temperature in 50 mM Tris-HCl buffer and 300 mM NaCl (pH 8.0). The two spectra were normalized to the Soret band of the nonenriched sE75 with the same absolute heme concentration (5.8 ± 0.4 μM).

Table 1: Spectral Properties and Heme Content of E75 LBD Mutants

LBD[a]	mutation	hemin[b]	Soret band (nm)	Rz[c]	% holoprotein[d]
wt	F370Y	−	424	0.7	11
wt	F370Y	+	424	2.4	99
s	H574A	+	419	0.6	11
s	C368A	+	422	1.6	39
s	C385A	+	424	1.5	37
s	C396A	+	422	2.3	89
s	C468A	+	424	1.0	20
s	C396A/C468A	+	414	0.1	nd[e]
s	C385A/C396A	+	422	1.2	24

[a] s stands for the soluble E75 LBD (F370Y). [b] Hemin (5 μM) added to the LB growth medium before cell induction. [c] Rz = A_{Soret}/A_{280}. [d] Percentages of holo forms, calculated from the absorbance at the Soret band and at 280 nm according to Experimental Procedures. [e] Not determined.

32 818 Da calculated from the amino acid sequence was checked by electrospray mass spectroscopy (data not shown).

Stoichiometry of Binding of Heme to sE75. The UV−visible spectrum of monomeric sE75 revealed a peak at 276 nm, a δ-peak at 359 nm, a Soret band at 424 nm, an α-peak at 575 nm, and a β-peak at 542 nm (Figure 3, gray line), suggesting a hexacoordinated ferric heme iron. The Reinheitszahl (Rz) (A_{Soret}/A_{280}) was 0.7 (Figure 3, gray line; Table 1). Addition of an excess of synthetic hemin (5 μM) to the purified protein did not modify the heme incorporation. By contrast, its addition upon cell lysis increased the Rz value 3-fold. Finally, when hemin (5 μM) was added to the LB medium during overexpression, the Rz reached its maximum value of 2.4 (Figure 3, black line; Table 1). Consequently, the sE75/heme stoichiometry was determined for monomeric sE75 overexpressed in the presence of hemin. The protoheme concentration of 24 ± 2 μM, determined by the pyridine hemochromogen assay, was found to be close to the sE75 concentration of 21 ± 1 μM, determined by quantitative amino acid analysis. This agrees well with the expected 1:1 stoichiometry (*6*) and indicates that the hemin-enriched sample is quantitatively a holoprotein. Consequently, these heme and sE75 concentrations were directly used to calculate the molar extinction coefficients of holo-sE75: $\epsilon_{424} = 105\,000\ M^{-1}\ cm^{-1}$ and $\epsilon_{280} = 44\,000\ M^{-1}\ cm^{-1}$. A theoretical ϵ_{280} of 14 815 $M^{-1}\ cm^{-1}$, corresponding to the apo form, was calculated from the sE75 amino acid sequence (ProtParam, ExPASy server). These molar extinction coefficients were then used to calculate the percentage of heme-bound protein (Table 1).

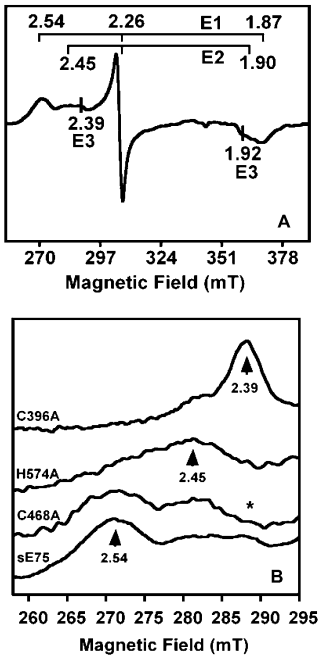

FIGURE 4: X-Band EPR spectra of heme-saturated sE75, wild type and mutants. (A) Spectrum in the $g \sim 2$ region of wild-type heme-saturated sE75. The apparent g values of the two major components (E1 and E2) are labeled, as well as the two extreme g values of the third component (E3). (B) Comparison of wild-type and mutant spectra in the $2.7 > g > 2.3$ region. The apparent g values of features are labeled. The asterisk indicates the disappearance of the $g = 2.39$ component in the C468A spectrum. Experimental conditions: buffer of 50 mM Tris-HCl, 300 mM NaCl, and 8% (v/v) glycerol (pH 8.0), modulation frequency of 100 kHz, modulation amplitude of 1 mT, microwave power of 1 mW, and temperature of 13 K.

EPR Spectroscopy of sE75. The EPR spectrum of the monomeric sE75 reflected heterogeneity in iron coordination. Indeed, this spectrum contained at least three overlapping sets of rhombic signals associated with g values corresponding to a low-spin ferric iron (Figure 4A and Table 2). No high-spin EPR signals were detected. Two components, here called E1 and E3, displayed well-defined lines. The third component displayed broad line widths with average g values of 2.45, 2.26, and 1.90, probably reflecting a distribution of

Table 2: EPR Parameters of sE75 and Mutants

sample	spin	comp[a]	%	g_1	g_2	g_3	V/Δ[b]	Δ/λ[c]
sE75	$^1/_2$	E1	35−50[d]	2.54	2.26	1.87	0.59	5.36
	$^1/_2$	E2	35−50[d]	2.45	2.27	1.90	0.46	5.85
	$^1/_2$	E3	∼5	2.39	2.26	1.92	0.35	6.33
H574A (pH 8)	$^1/_2$	E2	∼70	2.45	2.27	1.90	0.46	5.85
	$^5/_2$		∼30	7.97	3.59	∼2.0		
	$^5/_2$			6.90	5.13	∼2.0		
H574A (pH 9)	$^1/_2$	E2	>90					
	$^5/_2$		<10					
C396A	$^1/_2$	E2	<50	2.45	2.27	1.90	0.46	5.85
	$^1/_2$	E3	>50	2.39	2.26	1.92	0.35	6.33
C468A	$^1/_2$	E1	∼50	2.54	2.26	1.87	0.59	5.36
	$^1/_2$	E2	∼50	2.45	2.27	1.90	0.46	5.85

[a] Component of the EPR signal. [b] Rhombicity. [c] Tetragonal field. [d] Sample-dependent.

conformations that will be described collectively as E2. The absence (or very low content) of one of the sE75 EPR components in each mutant allowed *g* value identification. Deconvolution of the sE75 EPR spectrum was based on the relative intensities of E1−E3 in the H574A and C396A mutants (see below). The estimated contribution of each component to each spectrum is shown in Table 2. All *g* values are within the range found for thiolate hemoproteins (*20*−*23*) in which the cysteine ligand determines the EPR properties of the heme iron (*17*). In addition, the tetragonal field (Δ/λ) and rhombicity (V/Δ) parameters associated with E1−E3 depicted in Table 2 fit well in the "p-zone" of the Blumberg−Peisach diagram of CPO, P450, or eNOS proteins (Figure 7 of ref *24*). Multiple EPR low-spin signals have already been reported for several thiolate-ligated heme proteins (*20*). The EPR spectrum of sE75 also contains information about the nature of the sixth ligand, as previously demonstrated with P450 and CPO by a systematic study of the influence of the distal ligand (*22*). More precisely, the comparison of the *g* values depicted in Table 2 with published data (*22*) indicates that E1 probably corresponds to an N-donor iron ligand such as histidine (or imidazole). E2 is compatible with O-, N-, or S-donors (*25*−*27*). However, as shown below, the absorption spectrum data obtained from relevant mutants suggest that the hypothesis of an S-donor is unlikely. Because the *g* values of the E3, at the border limits of O- or S-donors (*22*), are inconclusive, further studies will be necessary to determine unambiguously the nature of this ligand.

Spectral Properties of Different Cysteine-to-Alanine Mutants. To better characterize the iron thiolate ligation (suggested by the EPR spectra), we mutated cysteines 368, 385, 396, and 468 (Figure 1) to alanine and studied their spectral properties. C385 and C396 were chosen because they are part of a Cys-Pro sequence known to be involved in heme responsive motifs (HRMs) (*15*). C468 and C368 were selected because they correspond to putative LBP residues (Figure 1). Two additional double mutants, C385A/C396A and C396A/C468A, were also made. All mutant proteins were overexpressed in the presence of hemin and subsequently purified. The UV−visible and EPR spectra of the C385A mutant were similar to those of wild-type sE75, although the former incorporated less heme (Table 1). This result indicates that C385 is not a ligand to the iron but is probably involved in stabilizing heme−protein interactions instead. EPR data from the C368A mutant were similar to

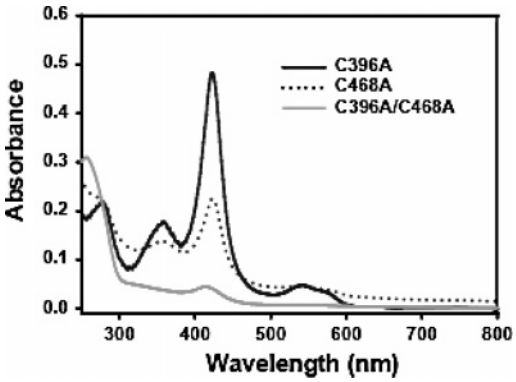

FIGURE 5: UV−visible spectra of cysteine mutants of sE75. The UV−visible spectra of cysteine mutants were recorded at room temperature in 50 mM Tris-HCl and 300 mM NaCl (pH 8.0): 5.3 μM C396A (black line), 10 μM C468A (dotted line), and 15 μM C396A/C468A (gray line).

sE75 except for a larger contribution of E2 at the expense of E1. This suggests that the C368 mutation destabilizes N-donor coordination and is consistent with the small blue shift of the Soret band from 424 to 422 nm (Table 1). The C396A mutant Soret band also shifted to 422 nm (Figure 5 and Table 1), but in contrast to that of the C368A mutant, its EPR spectrum was drastically modified with the disappearance of E1 and an increase in the level of E3 (Figure 4B and Table 2). The E2 signal was still present. Surprisingly, the *g* values of the C396A mutant were still characteristic of a thiolate iron ligand. This strongly suggests that C396 can be replaced with another cysteine. The C385A/C396A double mutation resulted in EPR and UV−visible spectra similar to those of the C396A mutant, confirming that C385 is not involved in heme iron binding, despite being part of a Cys-Pro sequence. On the other hand, C468 may contribute the alternative thiolate iron ligand. Although its Soret band at 424 nm is similar to that from sE75 (Figure 5 and Table 1), the EPR spectrum of the C468A mutant does not display E3 (Figure 4B and Table 2), a component that was predominant in the C396A mutant. We conclude from these results that (1) E3 reflects C468 coordination to the heme iron, which increases in the C396A mutant, and (2) E1 arises from C396/N-donor coordination, as this component was not observed in the C396A mutant EPR spectrum. The involvement of both C396 and C468 in iron coordination was confirmed by the C396A/C468A double mutation. Its UV−visible spectrum revealed a striking decrease in the magnitude of the Soret band combined with a significant shift to 414 nm (Figure 5 and Table 1). The limited solubility and the low heme iron content of this double mutant precluded further EPR studies.

Spectral Characterization of Histidine Mutants. Because E1 appears to be associated with a nitrogen-donor ligand to the iron, the four natural histidine residues of sE75 were successively mutated to alanine and all the proteins were overexpressed in the presence of hemin. The H364A mutant protein expression yield was too low to go beyond the IMAC column purification step and therefore to produce a protein solution devoid of free imidazole. Among the other three histidine mutants, only the H574A mutant displayed a UV−visible optical spectrum radically different from the one from sE75 (Figure 6A, gray line). The differences were (1) a strong decrease in the magnitude of the Soret band (Rz = 0.6 ±

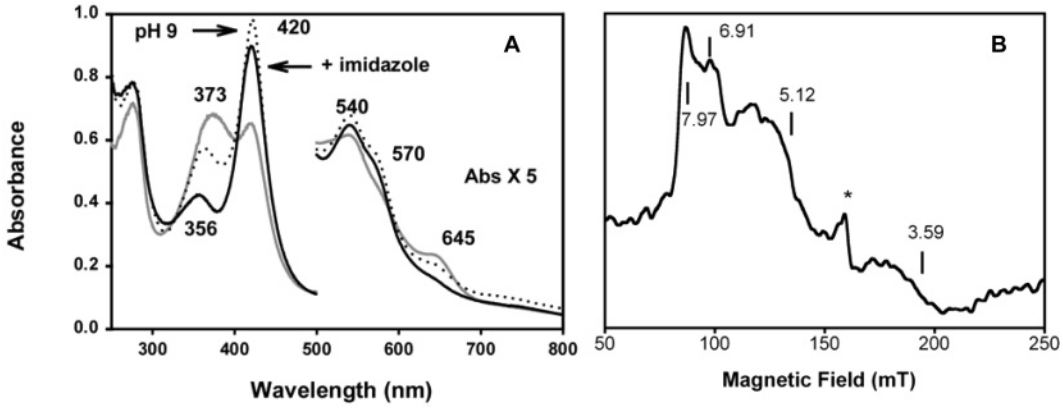

FIGURE 6: UV−visible absorption and X-band EPR spectra of the heme-saturated H574A mutant. (A) Effect of imidazole and pH on the UV−visible spectrum of the H574A mutant purified from a hemin (5 μM)-enriched *E. coli* culture: (gray line) 6.7 μM H574A in 50 mM Tris-HCl and 300 mM NaCl (pH 8.0), (black line) 6.7 μM H574A in 50 mM Tris-HCl, 300 mM NaCl (pH 8.0), and 300 mM imidazole, and (dotted line) 6.7 μM H574A in 50 mM Tris-HCl and 300 mM NaCl (pH 8.0, then adjusted to pH 9.0 by addition of small amounts of a 3.5 M Tris base solution). On the right side of the spectra is a 5-fold expanded absorbance scale for the 500−800 nm region. (B) EPR spectrum showing the low-field region ($g \sim 6$) of H574A. The asterisk indicates the nonspecific Fe^{3+} signal. Experimental conditions: buffer of 50 mM Tris-HCl, 300 mM NaCl, and 8% (v/v) glycerol (pH 8.0), modulation frequency of 100 kHz, modulation amplitude of 1 mT, microwave power of 1 mW, and temperature of 4 K.

0.2) with a small blue shift of the peak (from 424 to 419 nm), (2) a red shift of the δ-band from 359 to 373 nm, (3) a decrease in the magnitude of the α/β-bands (572 and 545 nm), and (4) the appearance of a CT1 band at 645 nm. Such an appearance of a CT1 band is indicative of the presence of high-spin Fe^{3+} (*28*). The H574A mutant has a heme content of only 11% (Table 1). Addition of imidazole to this protein resulted in an optical spectrum similar to that of sE75, differing only by the slight blue shift of several peaks (356, 420, 540, and 570 nm) (Figure 6A, black line). The EPR spectrum of the H574A mutant in the $g \sim 2$ region was characterized by the disappearance of E1, but an asymmetric absorption derivative signal with a $g_1 = 2.45$ maximum (Figure 4B) which corresponds to E2 was still observed. In addition, the EPR spectra revealed signals at low magnetic fields which confirm the presence of pentacoordinated high-spin Fe^{3+} (Figure 6B). The plurality of the high-spin components with two well-defined peaks at g values of 7.97 and 6.91, and other associated signals at g values of 3.59, 5.12, and ~2, probably reflects a diversity of iron ligands that are found for the low-spin components (see above). All g values, in the high and low magnetic fields, are in the range expected for Fe^{3+} with a thiolate ligand (*23*). Increasing the pH from 8 to 9 induced a shift of the high-spin states toward low-spin states (Table 2). This reduction of the high-spin signal from 30 to 10% reflects the binding of a sixth ligand. The UV−visible spectrum was also affected by the pH. It concerned mainly the δ-band whose magnitude was strongly decreased and shifted from 373 to 359 nm and the Soret band that was strongly increased in magnitude (Figure 6A). The absence of significant pH-dependent shift of the Soret band indicates that E2 very unlikely reflects a Cys/S-donor iron coordination. Indeed, it was shown that the 1-propanethiol complex of Fe^{3+} P450 displayed a pH-dependent absorption spectrum with an important red shift from 417 to 465 nm from pH 6.7 to 9, respectively (*29*). Because the spectrum of the H574A mutant at pH 9 is comparable to the absorption spectrum of the mutant in complex with imidazole (Figure 6A), the sixth ligand of E2 may be unprotonated imidazole coming from the IMAC chromatography purification step. Furthermore, as found with the N-donor complexes of P450 (*25*), the H574A mutant spectrum exhibited a stronger β-band than an α-band. However, the presence of an O-donor ligand, most probably derived from H_2O (although it can also be a tyrosine), cannot be ruled out even though in the O-donor complexes of P450 the α- and β-bands exhibited the same intensity (*25*).

DISCUSSION

Very recently, a heme prosthetic group was reported to be strongly bound to E75 with a 1:1 stoichiometry (*6*), but the heme iron coordination was not clearly elucidated. Mutation of surface residue F370 to tyrosine and addition of hemin to the growth medium before cell induction have allowed us to obtain a good yield of heme-enriched sE75 and to carry out EPR spectroscopy experiments. Three EPR conformations, E1−E3, were assigned to Cys/His, Cys/N(or O)-donor, and minor Cys/(non-N-donor) iron trans coordination, respectively. We conclude that E75 is a new member of the small Cys/His hemoprotein group. We have further studied heme iron coordination in E75 through site directed mutagenesis associated with EPR and UV−visible spectroscopies.

Heme Coordination. In this study, we have shown that H574 is the distal ligand in E1, confirming what was only suggested by a previous study (*6*). Rather surprisingly, we also found that the four cysteine-to-alanine mutants prepared in this study were capable of binding heme. The C396A mutant exhibited the most different EPR spectra compared to that of sE75, although it was still characteristic of a cysteine ligand and the heme content remained very high (Table 1). This indicates that another cysteine, identified as C468, on the basis of the C468A mutant EPR data, is also a ligand to the iron. The C396A/C468A double mutant, which did not significantly bind any hemin, confirmed that both residues can be involved in iron ligation. In contrast with preALAS-E (*15*), the second Cys-Pro sequence of E75 is not involved in heme binding as shown by the EPR data and UV−visible spectra of C368A and C368A/C396A mutants.

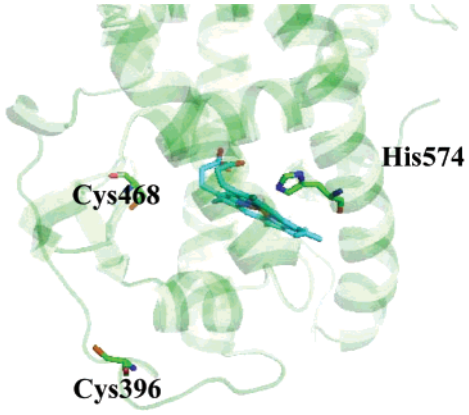

FIGURE 7: Positions of the E75 residues involved in heme iron coordination, in the canonical nuclear receptor structure. The hRARγ X-ray structure was used as a template. Heme was manually placed at the position corresponding to the RAR natural ligand using DeepView/Swiss-PDB Viewer.

Multiple low-spin EPR signals have already been reported for several thiolate-ligated heme proteins (*20*). Here, we have used site-directed mutagenesis to assign E1−E3 to specific pairs of heme iron ligands. Thus, E1 corresponds to C396/H574 coordination. The average E2 *g* value is indicative of a distal N-donor (however, an O-donor ligand cannot be ruled out) and may reflect a mixture of C396/N-donor and C468/N-donor coordination. The E3 component, absent from the C468A mutant, is associated with C468/X coordination. The nature of X could not be asserted because E3 was present in all the other mutants and its *g* value is borderline for both O- and S-donors. Theses results indicate that the distal His coordination (E1) is probably labile and can be replaced by the N or O-donor (E2 and E3) or S-donors (E3). The involvement of two cysteine thiolates in mutually exclusive iron coordination is surprising. It may result from the absence of the DBD, which renders the LBD more flexible than in the full-length protein. We believe that C396 is the natural cysteine iron ligand because its mutant exhibited the most striking modification of the EPR spectrum. However, the level of heme incorporation in the C396A mutant was unexpectedly high (Table 1), and consequently, our assignment can be only tentative. E78, a *Drosophila* nuclear receptor homologous to sE75 that contains a histidine at the position corresponding to H574, but no cysteines corresponding to either C396 or C468 (Figure 1), did not bind heme (data not shown). This observation underlies the predominant role of the two E75 LBD cysteine thiolates in the heme binding process. The three-dimensional helical structure and the positions of the residues involved in ligand binding are highly conserved in nuclear receptors. Consequently, we examined the putative positions of the E75 residues involved in heme iron coordination in the consensus structure. Figure 7 shows that H574 is in conserved helix H11, close to the LBP where the heme group should bind. In the consensus nuclear receptor model, C396 and C468 are far from the heme group (Figure 7). However, C396 is found in loop regions (Figure 7) with poorly conserved amino acid sequences (Figure 1) whose conformations are not likely to be conserved in the E75 structure.

Effect of Mutations on Heme Incorporation and Protein Stability. All mutations of residues not directly involved in heme iron binding reduced the level of heme incorporation (Table 1). For instance, only 41% of the C368A mutant molecules incorporated heme (Table 1). This residue probably belongs to the LBP, and the EPR data show that its mutation to alanine destabilizes the interaction between the heme iron and H574. The 23% level of heme incorporation in the C368A/C396A double mutant is likely to reflect the addition of the unfavorable effects of each single mutation. H364 belongs to the AHXXT motif responsible for the attachment of the H1 helix to the LBD core in many nuclear receptors (*30*). Consequently, the low yield of the H364A mutant is probably due to a destabilization of the E75 fold. In addition to its effect on heme iron coordination, the H574A mutation also destabilized the sE75 conformation. This is indicated by the fact that only 11% of the mutant molecules incorporated heme. This is much lower than the 40−55% level of heme incorporation that should result from the loss of histidine/iron coordination, as expected from the addition of E1 and E3 (Table 2).

E75 Is a New Cys/His Heme-Coordinated Protein. Only few natural Cys/His-coordinated heme proteins such as CBS (*16*), SoxAX (*17*), and HRI (*9*) have been characterized so far. As we have determined to be the case for sE75, the HRI Fe^{3+} tightly bound heme is coordinated to a cysteine thiolate on one side and to either a histidine or water trans to it. However, and in contrast to E75, a pentacoordinated iron was also detected in HRI. Although not generally accepted, the role of the heme in HRI may be that of a nitric oxide sensor (*9*). In their recent publication, Reinking and collaborators (*6*) showed that both NO and CO bind to E75 heme and that in vivo NO prevents the interaction of the nuclear receptor with DHR3. Consequently, they proposed that E75 may be a gas regulator of DHR3 transcriptional activation. Their published UV−visible spectral data show that, as found for HRI (*9*), binding of NO to the E75 LBD dissociates both heme Cys/His iron ligands, resulting in a Soret band at 391 nm. In contrast, when CO binds, the Soret band at 420 nm, characteristic of CO/His coordination, indicates that only the cysteine is dissociated. Assuming that NO is the natural heme gas ligand, it is conceivable that it induces the release of heme and consequently the E75 nuclear receptor conformational changes important for its regulatory role. However, heme could also be a hormone ligand to E75 in a more classical way without the need for NO binding. Our own results show that in E75 the heme iron is bound to C396, a residue that belongs to one of its two Cys-Pro sequences (*12*, *14*). It is well established that CP-containing HRMs regulate functions by simply binding heme as found, for instance, in the yeast HAP and the mammalian Bach1 transcription factors (*13*). In our hands, heme was incorporated at the cell lysis step, indicating that it can bind to newly synthesized apo-E75. This, in turn, may suggest that heme is not a structural or constitutive group as it would be required for a gas sensor, yet the two hypotheses are not conflicting since heme could regulate transcription by simply binding to apoE75 and subsequently be released from holoE75 when NO binds.

As reported for other nuclear receptors, E75 was very unstable in the absence of ligand. This instability was further demonstrated in the case of the H574A and C368A/C396A mutants that incorporated heme poorly and precipitated very shortly after purification. Because once purified, sE75 did not incorporate heme, it has not been possible to measure the dissociation constant and determine if it corresponds to

values typical of HMRs (micromolar) or to those of nuclear receptors (nanomolar). In any case, the affinity is probably very high because it is not possible to remove the heme by either heating or adding a denaturing agent (*6*). *Drosophila* E75 has been proposed to regulate expression of genes encoding enzymes involved in the ecdysteroid hormone biosynthetic pathway (*31*). In arthropods, ecdysteroids are generally synthesized by enzymes belonging to the cytochrome P450 family. One possible physiological role for E75 may be to regulate expression of one of these hemoprotein genes in response to variation in heme concentrations.

ACKNOWLEDGMENT

We thank Eugenie Carletti and Daniela Zaade, who as students from Université Joseph Fourier (Grenoble, France) contributed to this work, Claude Dauer (IGBMC, Illkirch, France) for cloning and providing the *E75-LBD* cDNA, and Delphine Blot for technical assistance. We are grateful to Bernard Dublet (IBS, Grenoble, France) for the MALDI mass spectrometry experiments and to Jean Pierre Mahy (LCBB, Orsay, France) and Elizabeth Lojou (BIP, Marseille, France) for helpful discussions.

REFERENCES

1. Renaud, J. P., and Moras, D. (2000) Structural studies on nuclear receptors, *Cell. Mol. Life Sci. 57*, 1748−1769.
2. White, K. P., Hurban, P., Watanabe, T., and Hogness, D. S. (1997) Coordination of *Drosophila* metamorphosis by two ecdysone-induced nuclear receptors, *Science 276*, 114−117.
3. Weatherman, R. V., Fletterick, R. J., and Scanlan, T. S. (1999) Nuclear-receptor ligands and ligand-binding domains, *Annu. Rev. Biochem. 68*, 559−581.
4. Falsone, S. F., Kurkela, R., Chiarandini, G., Vihko, P., and Kungl, A. J. (2001) Ligand affinity, homodimerization, and ligand-induced secondary structural change of the human vitamin d receptor, *Biochem. Biophys. Res. Commun. 285*, 1180−1185.
5. Moore, L. B., Goodwin, B., Jones, S. A., Wisely, G. B., Serabjit-Singh, C. J., Willson, T. M., Collins, J. L., and Kliewer, S. A. (2000) St. John's wort induces hepatic drug metabolism through activation of the pregnane X receptor, *Proc. Natl. Acad. Sci. U.S.A. 97*, 7500−7502.
6. Reinking, J., Lam, M. M., Pardee, K., Sampson, H. M., Liu, S., Yang, P., Williams, S., White, W., Lajoie, G., Edwards, A., and Krause, H. M. (2005) The *Drosophila* nuclear receptor e75 contains heme and is gas responsive, *Cell 122*, 195−207.
7. Ponting, C. P., and Aravind, L. (1997) PAS: A multifunctional domain family comes to light, *Curr. Biol. 7*, R674−R677.
8. Gilles-Gonzalez, M. A., and Gonzalez, G. (2005) Heme-based sensors: Defining characteristics, recent developments, and regulatory hypotheses, *J. Inorg. Biochem. 99*, 1−22.
9. Igarashi, J., Sato, A., Kitagawa, T., Yoshimura, T., Yamauchi, S., Sagami, I., and Shimizu, T. (2004) Activation of heme-regulated eukaryotic initiation factor 2α kinase by nitric oxide is induced by the formation of a five-coordinate NO-heme complex: Optical absorption, electron spin resonance, and resonance Raman spectral studies, *J. Biol. Chem. 279*, 15752−15762.
10. Lanzilotta, W. N., Schuller, D. J., Thorsteinsson, M. V., Kerby, R. L., Roberts, G. P., and Poulos, T. L. (2000) Structure of the CO sensing transcription activator CooA, *Nat. Struct. Biol. 7*, 876−880.
11. Omura, T. (2005) Heme-thiolate proteins, *Biochem. Biophys. Res. Commun. 338*, 404−409.
12. Lee, H. C., Hon, T., Lan, C., and Zhang, L. (2003) Structural environment dictates the biological significance of heme-responsive motifs and the role of Hsp90 in the activation of the heme activator protein Hap1, *Mol. Cell. Biol. 23*, 5857−5866.
13. Ogawa, K., Sun, J., Taketani, S., Nakajima, O., Nishitani, C., Sassa, S., Hayashi, N., Yamamoto, M., Shibahara, S., Fujita, H., and Igarashi, K. (2001) Heme mediates derepression of Maf recognition element through direct binding to transcription repressor Bach1, *EMBO J. 20*, 2835−2843.
14. Zhang, L., and Guarente, L. (1995) Heme binds to a short sequence that serves a regulatory function in diverse proteins, *EMBO J. 14*, 313−320.
15. Lathrop, J. T., and Timko, M. P. (1993) Regulation by heme of mitochondrial protein transport through a conserved amino acid motif, *Science 259*, 522−525.
16. Ojha, S., Hwang, J., Kabil, O., Penner-Hahn, J. E., and Banerjee, R. (2000) Characterization of the heme in human cystathionine β-synthase by X-ray absorption and electron paramagnetic resonance spectroscopies, *Biochemistry 39*, 10542−10547.
17. Cheesman, M. R., Little, P. J., and Berks, B. C. (2001) Novel heme ligation in a c-type cytochrome involved in thiosulfate oxidation: EPR and MCD of SoxAX from *Rhodovulum sulfidophilum*, *Biochemistry 40*, 10562−10569.
18. Rieske, J. S., Lipton, S. H., Baum, H., and Silman, H. I. (1967) Factors affecting the binding of antimycin A to complex 3 of the mitochondrial respiratory chain, *J. Biol. Chem. 242*, 4888−4896.
19. Schwede, T., Kopp, J., Guex, N., and Peitsch, M. C. (2003) SWISS-MODEL: An automated protein homology-modeling server, *Nucleic Acids Res. 31*, 3381−3385.
20. Pazicni, S., Lukat-Rodgers, G. S., Oliveriusova, J., Rees, K. A., Parks, R. B., Clark, R. W., Rodgers, K. R., Kraus, J. P., and Burstyn, J. N. (2004) The redox behavior of the heme in cystathionine β-synthase is sensitive to pH, *Biochemistry 43*, 14684−14695.
21. Lawson, R. J., Leys, D., Sutcliffe, M. J., Kemp, C. A., Cheesman, M. R., Smith, S. J., Clarkson, J., Smith, W. E., Haq, I., Perkins, J. B., and Munro, A. W. (2004) Thermodynamic and biophysical characterization of cytochrome P450 BioI from *Bacillus subtilis*, *Biochemistry 43*, 12410−12426.
22. Dawson, J. H., and Sono, M. (1987) Cytochrome p-450 and chloroperoxidase: Thiolate-ligated heme enzymes. Spectroscopic determination of their active-site structures and mechanistic implications of thiolate ligation, *Chem. Rev. 87*, 1255−1276.
23. Clark, R. W., Youn, H., Parks, R. B., Cherney, M. M., Roberts, G. P., and Burstyn, J. N. (2004) Investigation of the role of the N-terminal proline, the distal heme ligand in the CO sensor CooA, *Biochemistry 43*, 14149−14160.
24. Tsai, A. L., Berka, V., Chen, P. F., and Palmer, G. (1996) Characterization of endothelial nitric-oxide synthase and its reaction with ligand by electron paramagnetic resonance spectroscopy, *J. Biol. Chem. 271*, 32563−32571.
25. Dawson, J. H., Andersson, L. A., and Sono, M. (1982) Spectroscopic investigations of ferric cytochrome P-450-CAM ligand complexes. Identification of the ligand trans to cysteinate in the native enzyme, *J. Biol. Chem. 257*, 3606−3617.
26. Dhawan, I. K., Shelver, D., Thorsteinsson, M. V., Roberts, G. P., and Johnson, M. K. (1999) Probing the heme axial ligation in the CO-sensing CooA protein with magnetic circular dichroism spectroscopy, *Biochemistry 38*, 12805−12813.
27. Sigman, J. A., Pond, A. E., Dawson, J. H., and Lu, Y. (1999) Engineering cytochrome *c* peroxidase into cytochrome P450: A proximal effect on heme-thiolate ligation, *Biochemistry 38*, 11122−11129.
28. Neri, F., Indiani, C., Baldi, B., Vind, J., Welinder, K. G., and Smulevich, G. (1999) Role of the distal phenylalanine 54 on the structure, stability, and ligand binding of *Coprinus cinereus* peroxidase, *Biochemistry 38*, 7819−7827.
29. Sono, M., Andersson, L. A., and Dawson, J. H. (1982) Sulfur donor ligand binding to ferric cytochrome P-450-CAM and myoglobin. Ultraviolet−visible absorption, magnetic circular dichroism, and electron paramagnetic resonance spectroscopic investigation of the complexes, *J. Biol. Chem. 257*, 8308−8320.
30. Wurtz, J. M., Bourguet, W., Renaud, J. P., Vivat, V., Chambon, P., Moras, D., and Gronemeyer, H. (1996) A canonical structure for the ligand-binding domain of nuclear receptors, *Nat. Struct. Biol. 3*, 87−94.
31. Bialecki, M., Shilton, A., Fichtenberg, C., Segraves, W. A., and Thummel, C. S. (2002) Loss of the ecdysteroid-inducible E75A orphan nuclear receptor uncouples molting from metamorphosis in *Drosophila*, *Dev. Cell 3*, 209−220.
32. Renaud, J. P., Harris, J. M., Downes, M., Burke, L. J., and Muscat, G. E. (2000) Structure−function analysis of the Rev-erbA and RVR ligand-binding domains reveals a large hydrophobic surface that mediates corepressor binding and a ligand cavity occupied by side chains, *Mol. Endocrinol. 14*, 700−717.

BI060537A